

Anomal-E: A Self-Supervised Network Intrusion Detection System based on Graph Neural Networks

Evan Caville^{a,1,*}, Wai Weng Lo^{a,1,*}, Siamak Layeghy^a, Marius Portmann^a

^a*School of ITEE, The University of Queensland, Brisbane, Australia*

Abstract

This paper investigates Graph Neural Networks (GNNs) application for self-supervised intrusion and anomaly detection in computer networks. GNNs are a deep learning approach for graph-based data that incorporate graph structures into learning to generalise graph representations and output embeddings. As traffic flows in computer networks naturally exhibit a graph structure, GNNs are a suitable fit in this context. The majority of current implementations of GNN-based Network Intrusion Detection Systems (NIDSs) rely heavily on labelled network traffic which can not only restrict the amount and structure of input traffic, but also the NIDS' potential to adapt to unseen attacks. To overcome these restrictions, we present Anomal-E, a GNN approach to intrusion and anomaly detection that leverages edge features and graph topological structure in a self-supervised process. This approach is, to the best of our knowledge, the first successful and practical approach to network intrusion detection that utilises network flows in a self-supervised, edge leveraging GNN. Experimental results on two modern benchmark NIDS datasets not only clearly display the improvement of using Anomal-E embeddings, rather than raw features, but also the potential Anomal-E has for detection on wild network traffic.

Keywords: Graph Neural Network, Network Intrusion Detection System, Self Supervised, Graph Representation Learning, Anomaly Detection

1. Introduction

The increasing frequency and complexity of attacks on computer networks continue to threaten the security of information within computer systems. To combat this, enterprises utilise Network Intrusion Detection Systems (NIDSs) to protect critical infrastructure, data and networks. These systems commonly identify intrusions through the analysis of raw network traffic or flow-based records, traffic categorised with features detailing statistics about said flow. Traditionally, NIDSs can be broken into two main categories, signature-based and behavioural-based. Signature-based NIDSs utilise a pre-determined set of rules, metrics or calculations to address and classify network traffic. Behavioural NIDSs on the other hand rely on more complex operations, commonly involving Machine Learning (ML) to identify sophisticated and ever-evolving attacks. These behavioural specific approaches commonly use supervised learning, which is not always feasible as network traffic is rarely categorised, especially in the context of zero-day attacks. Furthermore, NIDS approaches have generally not considered the topological patterns of both benign and attack network traffic, which is an extremely important factor in network intrusion detection. Because of this,

we strongly argue for the inclusion of network flow topological patterns in NIDS development. This inclusion can be leveraged to detect sophisticated attacks such as advanced persistent threat (APT) attacks, as overall network graph patterns and lateral movement paths need to be considered.

Within this area, Graph Neural Networks are a promising recent development in deep learning with the ability to leverage topological patterns in training and testing. These neural networks take advantage of the graph structures through the use of messages passing between nodes and/or edges. This enables the neural network to learn and generalise effectively on graph-based data to output low-dimensional vector representations (embeddings) [1].

In this paper, we propose Anomal-E, a self-supervised GNN-Based NIDS. Given the severe lack of wild and labelled network traffic, it is difficult to train a supervised NIDS capable of detecting real network attacks. Therefore, to mitigate reliance on labelled data, Anomal-E utilises a self-supervised approach to intrusion detection. Furthering this, computer network traffic is naturally graph-based, as hosts represent nodes, and edges describe the flows or packets sent between them. Therefore, this is well suited for the graph-based, self-supervised network intrusion detection we present, without the need for data labels for zero-day attack detection.

Dominant graph-based learning approaches [2, 3] use only node/topological features and rely commonly on a random walks strategy which can lead to potentially important network flow information (edge information) being lost in the learning process. For NIDSs, network flow information is critical in

*Corresponding author

Email addresses: e.caville@uq.net.au (Evan Caville), w.w.lo@uq.net.au (Wai Weng Lo), siamak.layeghy@uq.net.au (Siamak Layeghy), marius@itee.uq.edu.au (Marius Portmann)

¹The first two authors contributed equally to this work.

identifying and mitigating network intrusions and anomalies. Thus, we propose Anomal-E to overcome this restriction and leverage graph information in a self-supervised learning manner. Anomal-E consists of two main components; the first component is E-GraphSAGE [4]. E-GraphSAGE extends the original GraphSAGE [2] model to capture edge features and topological patterns in graphs. The second critical component in Anomal-E is the modified Deep Graph Infomax (DGI) method [5], which maximises the local mutual edge information between different parts of the input in the latent space for self-supervised learning.

Anomal-E is specifically designed and implemented for the problem of network intrusion detection. The unique combination of its two key components allows for a completely self-supervised approach to the generation of edge embeddings without using any data labels; the generated edge embeddings can then be fed to any traditional anomaly detection algorithms, such as Isolation Forest (IF) [6], for network intrusion detection.

To the best of our knowledge, our approach is the first thoroughly analysed, evaluated, practical and successful approach to designing self-supervised GNNs for the problem of network intrusion detection.

In summary, the key contributions of this paper are:

- We propose Anomal-E, a self-supervised GNN-based approach for network intrusion detection. The proposed method allows the incorporation of both edge features and topological patterns to detect attack patterns by itself without the need for any data labels.
- The proposed Anomal-E is based on E-GraphSAGE, modified DGI and four different traditional anomaly detection algorithms, namely, PCA-based anomaly detection (Principal Component Analysis) [7], IF, Clustering Based Local Outlier Factor (CBLOF) [8] and Histogram-based Outlier Score (HBOS) [9], for network intrusion detection. Our proposal is the first to utilize self-supervised GNNs for network intrusion detection, to the best of our knowledge.
- We applied Anomal-E on two benchmark NIDS datasets for network intrusion detection, where significant improvements over raw features demonstrated its potential via extensive experimental evaluation.

The rest of the paper is organized as follows. Section 3 discusses background, and Section 2 provides an overview of the key related works. Our proposed Anomal-E algorithm and the corresponding NIDS are introduced in Section 4. Experimental evaluation results are presented in Section 5, and Section 6 concludes the paper.

2. Related Work

As the work we present utilises current methods at the forefront of GNNs and applies them to network anomaly detection in a self-supervised context, there is a very limited amount of

prior work, that we know of, that is very closely related to our research. Therefore, the prior research discussed below relates to our approach in a more broad sense.

Casas et al. [10] propose an unsupervised NIDS utilising Sub-Space Clustering, DBSCAN and Evidence Accumulation (EA4RO). Sub-space clustering enables feature vectors to be projected into k-dimensional sub-spaces, where each sub-space is then grouped by DBSCAN algorithms. Due to DBSCAN's use of density to identify clusters, anomalies were located in the low-density clusters. Finally, EA4RO is applied for calculating the degree of dissimilarity from the outlier to the centroid of the largest cluster, using the Mahalanobis distance as the metric. This proposed algorithm is evaluated using the KDD'99 dataset and achieved 100% accuracy. However, this dataset is over two decades old and does not reflect the current sophistication of network attacks.

In [11], authors studied and compared the performances of various anomaly detection-based methods including the k-medoids, k-means, EM and distance-based algorithms for unsupervised network intrusion detection. Experiments were evaluated using the NSL-KDD dataset. This dataset is an improved version of the KDD'99 dataset, solving redundant problems as about 78% of the records are duplicated in the training set and and 75% are duplicated in the test set. Overall, they achieved 78.06% accuracy in the EM clustering approach, 76.71% accuracy using k-Medoids, 65.40% when using improved k-Means and 57.81% using k-Means. However, all algorithms used in the experiments suffer from high false-alarm rates (FAR), with an overall rate of 20% achieved across all four algorithms.

Leichtnam et al. [12] defined a security object graph and applied an autoencoder (AE) model to perform network intrusion detection in an unsupervised manner. The authors evaluated the proposed model performances on the CICIDS2017 dataset and reported that they can achieve a binary classification performance with an F1-Score of 0.94 and classification accuracy of 97.481

Monowar H. Bhuyan et al. [13] proposed a tree-based sub-space clustering technique to find clusters among intrusion detection data, without using labels. The network data was however labelled using a clustering technique based on a TreeCLUS algorithm. This proposed method works faster for detecting intrusions in the numeric mixed categories of network data.

Layeghy et al. [14] investigated the performance and ability of generalisation of ML-based NIDSs by comprehensively evaluating seven different supervised and unsupervised machine learning algorithms on four recently published benchmark NIDS datasets. For the unsupervised learning experiments, IF, One-Class Support Vector Machines (oSVM), and Stochastic Gradient Descent one-Class Support Vector Machines (SGD-oSVM) were considered. Overall, the results demonstrated that unsupervised anomaly detection algorithms can generalise better than supervised learning methods.

[15][16] proposed a traditional graph embedding approach to perform network intrusion detection. They first converted the network flows into network graphs based on source and destination IP and Port pairings and then applied traditional graph embedding techniques such as DeepWalk (skip-gram) for net-

work intrusion detection. However, a significant limitation of this approach is the application of traditional transductive graph embedding methods [17], which cannot generalise to any unseen node embeddings, e.g. IP addresses and port numbers, not included during the training phase. This makes the approach unsuitable for most practical NIDS application scenarios, as we cannot expect every IP and port pair to appear in the training data.

Zhou *et al.* [18] propose a GNN model for end-to-end botnet detection. In this approach, the authors consider only the topological structure of the network rather than the features associated with each node and edge. To simulate a realistic network, authentic background traffic is embedded into existing benchmark botnet datasets. In order to focus on only topological structure, edge features were omitted and node features are set to an all-one constant vector. This enables for the model to aggregate features throughout the graph without any consideration or effects from unique node attributes. The authors used this approach to graph learning to formulate a binary classification problem to identify botnets. They found that their proposed model significantly improved botnet detection when compared to results achieved by logistic regression and the existing botnet detection tool, BotGrep [19].

3. Background

Graph representation learning is a fast growing area of research that can be applied to various applications such as telecommunication and molecular networks. Recently, GNNs have achieved state-of-the-art performance in cyberattack detection, such as network intrusion detection [4, 20].

3.1. Graph Neural Networks

GNNs at a very high level can be described as a deep learning approach for graph-based data and a recent, highly promising area of ML. GNNs essentially acts as an extension to convolutional neural networks (CNNs) that can generalise to non-euclidean data [1, 21]. A key feature of GNNs is their ability to use the topological graph structure to their advantage through message passing. For each node in a graph, this means aggregating neighbouring node features to leverage a new representation of the current node that takes into account neighbouring information [22]. The output of this process is known as embeddings [23]. For nodes, embeddings are low or n-dimensional vector representations that capture topological and node properties. This process can be performed for edges and graphs in a similar fashion to output edge and graph embeddings. Embeddings are then commonly used for both supervised and unsupervised downstream tasks e.g node classification, link prediction and anomaly detection.

As computer networks and their traffic flows are naturally able to be represented in graph form, the application of GNNs for network intrusion and anomaly detection is a promising approach for detecting new and advanced network attacks, such as APT attacks. In this context, nodes can be represented by IP addresses. Edges then are represented by the communication of packets or flow between nodes [24].

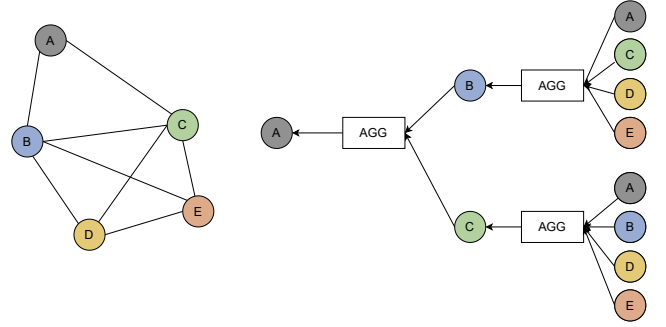


Figure 1: Two-hops Graph Convolutional Networks with full neighbourhood sampling technique

3.2. GraphSAGE

Graph Sample and aggregatE (GraphSAGE) is one of the state-of-the-art graph neural network models proposed by Hamilton *et al.* [17]. In GraphSAGE, a neighbour sampling technique can be applied to sample a fixed-size subset of node neighbours for neighbour message propagation. The neighbour sampling aims to minimizing the size of the computational graph to reduce the space and time complexity of the algorithm.

The GraphSAGE algorithm performs graph convolutional operations on a graph $\mathcal{G}(\mathcal{V}, \mathcal{E})$, where nodes represent as \mathcal{V} and edges represent as \mathcal{E} and x_v represent node features.

For specifying the depth of the graph neural networks, a k -hop neighbourhood needs to be set, which represents k -hop node neighbour information need to be aggregated at each iteration. Another important aspect is the choice of a differentiable aggregator function $AGG_k, \forall k \in \{1, \dots, K\}$ for neighbour information aggregation. In GraphSAGE, various aggregation methods can be applied, including mean, pooling, or different types of neural networks, e.g., Long Short-Term Memory (LSTM) [17].

3.2.1. Node Embedding

For each node, the GraphSAGE model iteratively aggregates k -hop neighbour information. At each iteration, a set of the neighbour's nodes can be sampled to reduce the space and time complexity, and the representation from the sampled nodes is aggregated for generating node embeddings.

At the k -th layer, the aggregated node neighbour information $\mathbf{h}_{\mathcal{N}(v)}^k$ at a node v , based of the sampled neighborhood $\mathcal{N}(v)$, can be expressed as Equation 1 [17]:

$$\mathbf{h}_{\mathcal{N}(v)}^k = AGG_k(\{\mathbf{h}_u^{k-1}, \forall u \in \mathcal{N}(v)\}) \quad (1)$$

Here, the node embedding \mathbf{h}_u^{k-1} indicates as node embedding u in the previous layer. These neighbour node embeddings are aggregated into the embedding of node v at layer k .

This aggregation process is illustrated in Figure 1 (right); the k -hop neighbourhood node features of each graph node are aggregated based on the aggregation function.

The aggregated representation from the sampled neighbours is then concatenated with the node representation of itself \mathbf{h}_v^{k-1} . After that, the model weights \mathbf{W}^k can be applied and the result

Algorithm 1: E-GraphSAGE edge embedding [4]

input : Graph $\mathcal{G}(\mathcal{V}, \mathcal{E})$;
input edge features $\{\mathbf{e}_{uv}, \forall uv \in \mathcal{E}\}$;
input node features $\mathbf{x}_v = \{1, \dots, 1\}$;
depth K ;
weight matrices $\mathbf{W}^k, \forall k \in \{1, \dots, K\}$;
non-linearity σ ;
differentiable aggregator functions AGG_k ;

output: Edge embeddings $\mathbf{z}_{uv}, \forall uv \in \mathcal{E}$

```
1  $\mathbf{h}_v^0 \leftarrow \mathbf{x}_v, \forall v \in \mathcal{V}$ 
2 for  $k \leftarrow 1$  to  $K$  do
3   for  $v \in \mathcal{V}$  do
4      $\mathbf{h}_{\mathcal{N}(v)}^k \leftarrow AGG_k(\{\mathbf{h}_u^{k-1} \parallel \mathbf{e}_{uv}^{k-1}, \forall u \in \mathcal{N}(v), uv \in \mathcal{E}\})$ 
5      $\mathbf{h}_v^k \leftarrow \sigma(\mathbf{W}^k \cdot \text{CONCAT}(\mathbf{h}_v^{k-1}, \mathbf{h}_{\mathcal{N}(v)}^k))$ 
6    $\mathbf{z}_v = \mathbf{h}_v^K$ 
7   for  $uv \in \mathcal{E}$  do
8      $\mathbf{z}_{uv}^k \leftarrow \text{CONCAT}(\mathbf{z}_u^k, \mathbf{z}_v^k)$ 
9 return  $\mathbf{z}_{uv}^K, \mathbf{z}_v$ 
```

is passed to a non-linear activation function σ (e.g. ReLU), for obtaining the final node embeddings \mathbf{h}_v^k , as shown in Equation 2 [17].

$$\mathbf{h}_v^k = \sigma(\mathbf{W}^k \cdot \text{CONCAT}(\mathbf{h}_v^{k-1}, \mathbf{h}_{\mathcal{N}(v)}^k)) \quad (2)$$

Thus, the final node representation of node v can be represented as \mathbf{z}_v , which represents the node embeddings at the final layer K , as shown in Equation 3. For the purpose of node classification, the node embeddings (node representation) \mathbf{z}_v can be fed to a sigmoidal neuron or softmax layer for the node classification task.

$$\mathbf{z}_v = \mathbf{h}_v^K, \quad \forall v \in \mathcal{V} \quad (3)$$

3.3. E-GraphSAGE

Graph neural networks have been successfully applied in various application domains. However, these approaches mainly focus on node features for message propagation and are currently unable to consider edge features for edge classification. Therefore, the E-GraphSAGE algorithm was proposed to capture k-hop edge information for generating edge embeddings for network intrusion detection. This provides the basis for computing the corresponding edge embeddings and enabling edge classification; that is, the classification of computer network flows into benign and attack flows.

The goal of an NIDS is essentially to detect malicious network flows. The problem can therefore be formulated as an edge classification problem in graph representation learning.

The original GraphSAGE algorithm only considers node features for message information propagation rather than edge features [17]. However, most network attack datasets only consist of network flow features. Thus, the algorithm is required to sample and aggregate the k-hop edge features of the graph. Also, the final output of the algorithms should be edge embeddings for malicious network flow detection, rather than node embeddings. As a result, the E-GraphSAGE algorithm was proposed with these modifications, as shown in Algorithm 1.

The main differences when comparing the original GraphSAGE algorithm [17] with E-GraphSAGE, are the algorithm inputs, the message propagation function, and the algorithm outputs.

The algorithm input should include edge features $\{\mathbf{e}_{uv}, \forall uv \in \mathcal{E}\}$ for edge feature message propagation, which is missing from the original GraphSAGE. Since all the network intrusion detection datasets only consist of edge features, hence network flow features rather than node features are critical. Therefore, the algorithm is only using edge features (network flow) features for network intrusion detection. To initialize the node representation, $\mathbf{x}_v = \{1, \dots, 1\}$ has been used to initialize the node features, and the dimension of all initial all-one constant vector is the same as the number of edge features, as shown in Line 1 of the algorithm.

In Line 4, to perform neighbour information aggregation based on edge features rather than node features, a new neighborhood aggregator function was proposed to create the *aggregated edge features of the sampled neighborhood edges and neighbour information* at the k -th layer, as shown in Equation 4 below.

$$\mathbf{h}_{\mathcal{N}(v)}^k \leftarrow AGG_k(\{\mathbf{h}_u^{k-1} \parallel \mathbf{e}_{uv}^{k-1}, \forall u \in \mathcal{N}(v), uv \in \mathcal{E}\}) \quad (4)$$

Here, \mathbf{e}_{uv}^{k-1} are represented as edge features uv from $\mathcal{N}(v)$, the sampled neighborhood of node v , at layer $k-1$. The aggregated edge features can be concatenated with neighbour node embeddings \mathbf{h}_u^{k-1} for edge feature message propagation. In Line 5, the node embedding for node v at layer k based on k-hop edge features is computed, and the neighbour node embedding consists of the neighbour edge features. Thus, the k-hop edge features and topological patterns in the graph are collected and aggregated, and can be combined with the self node representation \mathbf{h}_v^{k-1} .

The final node representations at depth K , $\mathbf{z}_v = \mathbf{h}_v^K$, are computed in Line 6. The final edge embeddings \mathbf{z}_{uv}^K for each edge uv are computed as the concatenation of a pair of node embeddings, u and v , as shown in Equation 5 below.

$$\mathbf{z}_{uv}^K = \text{CONCAT}(\mathbf{z}_u^K, \mathbf{z}_v^K), uv \in \mathcal{E} \quad (5)$$

This represents the final output of the forward propagation stage in E-GraphSAGE.

3.4. Deep Graph Infomax

Deep Graph Infomax (DGI) [26] is a self-supervised graph-based learning approach that aims to train an encoder to learn node representations by maximising mutual information between patch representation and global representation. Fig. 2 shows the overall process of DGI to perform mutual information maximisation. Here, G represents the input graph used, and E represents the encoder. In order to train this encoder, a corrupted graph H is first created through the use of a corruption function, C .

As DGI focuses on node representations within the graph, the corruption function (i.e. random permutation of the input graph node features which add or remove edges from the adjacency matrix A) needs to be defined to generate corrupted

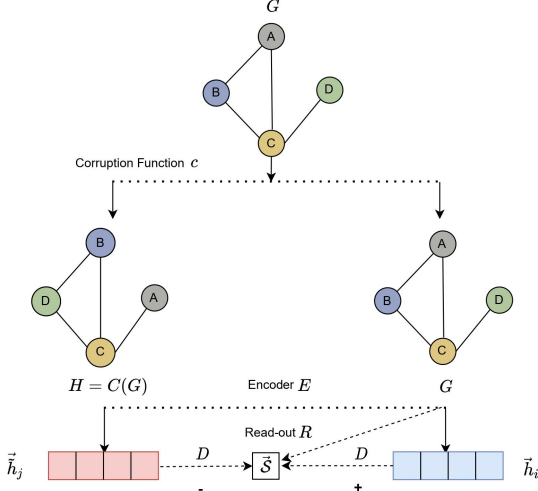


Figure 2: High-level overview of the DGI model [25]

graphs. These graphs are then passed into the encoder E , which any existing GNN, e.g GraphSAGE, can represent. The encoder then outputs node embeddings of the input graph sample G , and the negative graph sample H .

With the input graph embeddings G , a global graph summary \vec{s} is produced using a readout function R . \vec{s} represents the summary of the input graph calculated by averaging all the given node embeddings and passing them through a sigmoid function. Finally, both the input graph embeddings \vec{h}_i , and negative sample embeddings \vec{h}_j , are evaluated through the use of a discriminator D . The discriminator uses the input graph and negative graph embeddings to score them against the global graph summary using a simple bilinear scoring method. By scoring these embeddings using the global graph summary, DGI achieves its goal in maximising the mutual local-global information and can update the parameters in D , R and E , using gradient descent to continue training the encoder.

4. Anomal-E

Figure 3 displays an overview of the anomaly detection process performed using Anomal-E. Firstly, raw network flows are pre-processed to generate representative training and testing graphs. The training graph is then fed into the Anomal-E training process to train the E-graphSAGE encoder. By using E-GraphSAGE, Anomal-E aims to learn edge representations that maximise local-global mutual information in a self-supervised context. Similar to the DGI methodology, a negative graph representation is first generated using a corruption function. However, rather than generating a random permutation of the input graph’s node features, edge features are randomly permuted instead. Both these graphs are then passed through the E-GraphSAGE encoder. E-GraphSAGE then outputs the edge embeddings of the input graph and negative graph. As with the original DGI methodology, these embeddings are used to generate a global graph summary that the input and negative embeddings can be scored against using a discriminator. Now,

Algorithm 2: Pseudocode of Proposed Anomal-E Algorithm

input : Graph $\mathcal{G}(\mathcal{V}, \mathcal{E}, \mathcal{A}, \mathcal{X})$;
Input edge features $\{\mathbf{e}_{uv}, \forall uv \in \mathcal{E}\}$;
Input node features $\mathbf{x}_v = \{1, \dots, 1\}$;
Depth K ;
Number of training epochs T ;
Corruption function C ;

output: Optimized E-GraphSAGE encoder g ,
Optimized PCA h_PCA , Optimized Isolation Forest h_IF , Optimized CBLOF h_CBLOF , Optimized HBOS h_HBOS

- 1 Initialize the parameters θ and ω for the encoder g and the discriminator D ;
- 2 **for** $epoch \leftarrow 1$ to T **do**
- 3 $\mathbf{z}_{uv}^K, \mathbf{z}_v^K = g(\mathcal{G}, \theta)$
- 4 $\tilde{\mathbf{z}}_{uv}^K, - = g(C(\mathcal{G}), \theta)$
- 5 $\bar{s} = \sigma\left(\frac{1}{n} \sum_{i=1}^n \mathbf{z}_v^{K^T}\right)$
- 6 $\mathcal{D}(\mathbf{z}_{uv}^K, \bar{s}) = \sigma(\mathbf{z}_{uv}^K \mathbf{w} \bar{s})$
- 7 $\mathcal{D}(\tilde{\mathbf{z}}_{uv}^K, \bar{s}) = \sigma(\tilde{\mathbf{z}}_{uv}^K \mathbf{w} \bar{s})$
- 8 $\mathcal{L}_{DGI} =$
 $-\frac{1}{2n} \sum_{i=1}^n (\mathbb{E}_G \log \mathcal{D}(\mathbf{z}_{uv}^K, s) + \mathbb{E}_G \log (1 - \mathcal{D}(\tilde{\mathbf{z}}_{uv}^K, s)))$
- 9 $\theta, \omega \leftarrow \text{Adam}(\mathcal{L}_{DGI})$
- 10 $\mathbf{z}_{uv}^K, - = g(\mathcal{G}, \theta)$
- 11 $h_IF \leftarrow \text{IF}(\mathbf{z}_{uv}^K)$
- 12 $h_PCA \leftarrow \text{PCA}(\mathbf{z}_{uv}^K)$
- 13 $h_CBLOF \leftarrow \text{CBLOF}(\mathbf{z}_{uv}^K)$
- 14 $h_HBOS \leftarrow \text{HBOS}(\mathbf{z}_{uv}^K)$
- 15 **return** $h_IF, h_PCA, h_CBLOF, h_HBOS, g$

parameter adjustment occurs using these scores and the process is repeated to continue training the E-graphSAGE encoder. Once training is complete, the output training graph embeddings are used to train four different existing anomaly detection algorithms. Detection accuracy is then determined through inputting the testing graph through these algorithms. These steps are explained in further detail in the following sections.

4.1. Algorithm Description

Anomal-E can be represented in Algorithm 2. For training the proposed model, the input includes the network graph \mathcal{G} with network flow features to extract true edge embeddings and corrupted edge embedding embeddings. Before this, we need to define the corruption function C to generate the corrupted network graphs $C(\mathcal{G})$ for E-GraphSAGE to extract the corrupted edge embeddings. In this paper, we randomly shuffled the edge features among the edges in real network graphs \mathcal{G} to generate the corrupted network graphs. This is done by shuffling the edge feature matrix in rows \mathbf{X} . Overall, instead of adding or removing edges from the adjacency matrix such that $(\tilde{\mathbf{A}} \neq \mathbf{A})$, we use corruption function C which shuffles the edge features such that $(\tilde{\mathbf{X}} \neq \mathbf{X})$, but retain the adjacency matrix $(\tilde{\mathbf{A}} = \mathbf{A})$.

For each training epoch, Line 3 to 4, we use E-GraphSAGE to extract true edge embeddings, true global graph summaries and corrupted edge embeddings; rather than having a 2-layer E-GraphSAGE model, a 1-layer model is used. This is because the base DGI model benefits from wider rather than deeper models.

In Line 5 to 6, for the discriminator \mathcal{D} , we introduced the non-linear logistic sigmoid function, which compares the edge

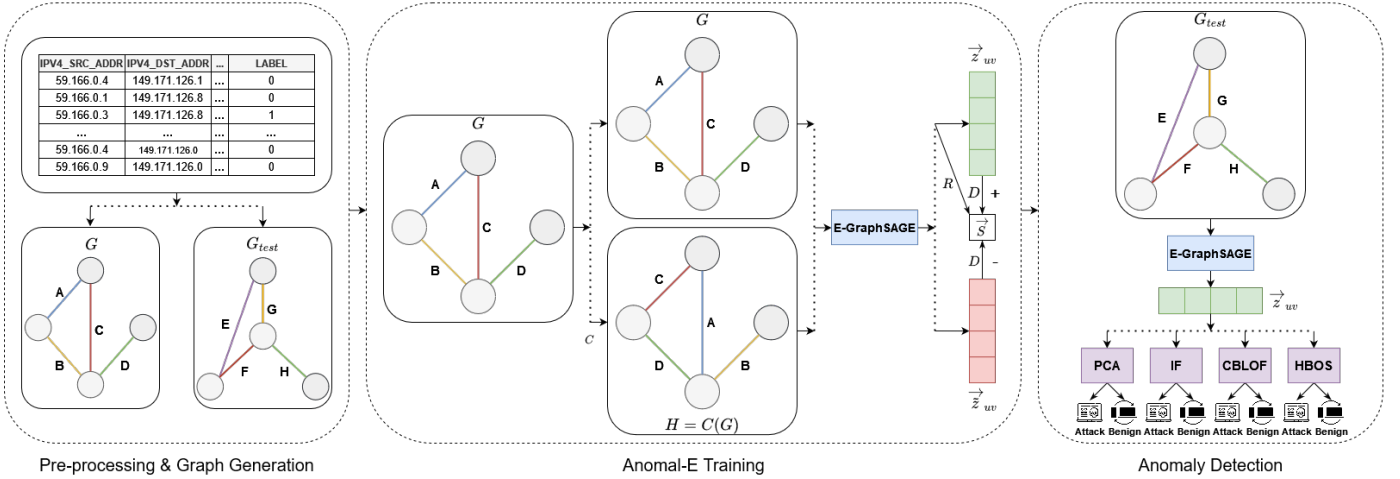


Figure 3: Proposed Anomal-E NIDS pipeline. A given a flow-based dataset is pre-processed into training and testing graphs where endpoints represent nodes and flows are the edges between them (left). The training graph is used to then train the Anomal-E model in which positive and negative embeddings are generated and used to tune and optimise the E-GraphSAGE model (middle). Finally, test embeddings are generated from the tuned E-GraphSAGE model to use in downstream anomaly detection algorithms (right).

embedding vector \bar{z}_{uv} against a real whole graph embedding \bar{s} to calculate the score of (\bar{z}_{uv}, \bar{s}) being positive or negative.

$$\mathcal{D}(\mathbf{z}_{uv}^K, \bar{s}) = \sigma(\mathbf{z}_{uv}^{K^T} \mathbf{w} \bar{s}) \quad (6)$$

$$\mathcal{D}(\bar{\mathbf{z}}_{uv}^K, \bar{s}) = \sigma(\bar{\mathbf{z}}_{uv}^{K^T} \mathbf{w} \bar{s}) \quad (7)$$

We then applied a binary cross-entropy loss objective function to perform gradient descent, as shown Line 8. To perform gradient descent, we maximize the score if the edge embedding is a true edge embedding \bar{z}_{uv} and minimize the score if it is a corrupted edge embedding \bar{z}_{uv} compared to the global graph summary generated by the read-out function \mathcal{R} . As a result, we can maximize the mutual information between patch representations (i.e. edge representations) and the whole real graph summary. After the training process, the trained encoder can be used to generate new edge embeddings for downstream purposes, i.e. anomaly detection. Finally, in line 11 to 14 we applied various anomaly detection algorithms including PCA, IF, CBLOF and HBOS for unsupervised anomaly detection.

4.2. Pre-processing & Graph Generation

Netflow data allows for a seamless integration of flow records into graph format as nodes can be represented through IP addresses and/or ports and flow information naturally represents edges. Figure 4 shows an overview of the process undertaken to pre-process Netflow records from each dataset into training and testing graphs. For experiments in this study, source and destination port information is firstly removed from each flow record. The data is then downsampled to 10% of its original size, similar to that seen in [27]. On downsampled flows, samples are separated into training and testing sets. Target encoding on categorical features in both the training and testing set then occurs. To perform this is an unsupervised manner, the training set is used to train a target encoder on categorical data, to which encoding is performed again using

the fully trained encoder on both the training and testing set. Any empty or infinite values arisen from this process is then replaced with a value of 0. Before finally generating graphs, training and testing sets are then normalised using an L2 normalisation approach. Similarly to the approach taken in target encoding, the normaliser is trained using the training set to ensure an unsupervised process is achieved. Finally, the training and testing sets are converted into bidirectional graph representations. Processed flow information is then applied as edge features. Additionally, following the E-GraphSAGE methodology, each graph's node features are set to a constant vector containing ones with the same dimensions to that of the edge features i.e if 49 edge features are used, node features will be vectors of 49 ones.

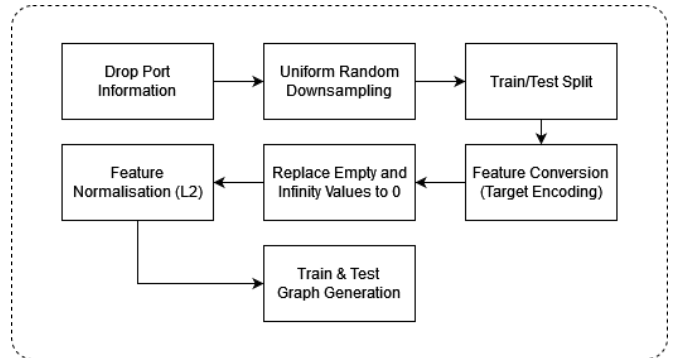


Figure 4: Pre-processing & Graph Generation Method

4.3. Training

For each dataset and experiment, training occurs using the generated training graph as discussed previously. Before training commences in the Anomal-E model, multiple components are required to be set and configured. Firstly, the encoder is set to E-GraphSAGE. The encoder uses a mean aggregation

function and uses similar hyperparameters to the authors' approach in their paper however, rather than having a 2-layer E-GraphSAGE model, a 1-layer model is used. To summarise, the encoder uses a hidden layer size of 128 units which also matches the final output layer size. However, as the encoder generates edge embeddings, this size is doubled to 256. ReLU is used for the activation function and no dropout rate is included. As for the generation of the global graph summary, the same approach used by authors in the DGI paper is used. However, instead of averaging node embeddings and passing them through a sigmoid function, edge embeddings are used. A binary cross entropy function is used to calculate loss and gradient descent is used for backpropagation with the Adam optimiser using a learning rate of 0.003.

4.4. Anomaly Detection

Upon completion of training, the parameter tuned E-GraphSAGE model is used to generate edge embeddings from both the training and testing graph. To perform the anomaly detection process, the 4 algorithms mentioned previously are considered. To train each algorithm in an unsupervised manner, edge embeddings generated from the training graph are used as inputs. Contaminated and non-contaminated training samples are also considered in experiments i.e training with attack samples omitted and training with attack samples included. Grid searches are also performed in each experiment for each detection algorithm to ensure optimal parameter tuning. In particular, all algorithms are grid searched on the contamination parameter along with number of components, number of estimators, number of clusters and number of bins parameter for PCA [7], IF [6], CBLOF [8] and HBOS [9] respectively. Once each algorithm is trained, the test edge embeddings are then used to evaluate the success of the model in an unsupervised fashion as seen in the "Anomaly Detection" phase in Figure 3.

It is important to note that the PCA-based algorithm [7] used at this stage for anomaly detection is an extension of the regular PCA algorithm, adapted for anomaly detection rather than dimensionality reduction. This method first performs a PCA reduction on a set of "normal" samples to extract a correlation matrix. This "normal" correlation matrix then acts a criterion for the outlier detection stage of the algorithm, i.e. if a sample deviates to a certain degree from this normal, it is considered an outlier. In this paper, we refer to this extension of the PCA algorithm simply as PCA.

As for IF anomaly detection [6], tree structures are leveraged to isolate and identify samples that represent anomalies. If a sample is isolated closer to the root of the tree, then it is identified as an anomaly, and samples deeper in the tree are determined as "normal". This process is built through an ensemble of trees to create an Isolation Forest. This commonly used algorithm is found to effectively and accurately identify anomalies at an efficient rate.

The CBLOF [8] algorithm approaches anomaly detection as a clustering-based problem. Samples are clustered and given an outlier-factor that represents both the size of the cluster the sample belongs to, as well as the distance between itself and the nearest cluster. This factor defines the degree of variation

the sample has which is used to determine if it is an anomaly or not.

HBOS [9] on the other hand takes a histogram-based approach to anomaly detection rather than the cluster-based approach taken for CBLOF. In this method, univariate histograms are constructed for each feature with each histogram containing a set of bins. The frequency of slotted samples in each bin for each histogram enables for bin densities to be derived. The density value calculated for each histogram is then used to determine the HBOS score to dictate whether a sample is an outlier.

5. Experiments and Results

For the performance evaluation of Anomal-E, multiple testing approaches are considered. As labelled datasets are used in this paper, both datasets' contamination and non-contamination is investigated and evaluated against multiple standard anomaly detection algorithm. Datasets are randomly and uniformly downsampled to 10% considering the large size of their original representations. In training, 70% of data is used. Once complete, the remaining 30% of samples are used for testing and performance evaluation.

To clearly distinguish the difference and benefit of using Anomal-E embeddings in anomaly detection, our results compare Macro F1-scores between using raw features and Anomal-E embeddings as anomaly detection algorithm inputs. Macro F1-Scores are used as a key performance indicator throughout our experiments, as this metric combats the problem of potential imbalance within datasets.

5.1. Datasets

2 benchmark NIDS datasets are used in our experiments: NF-UNSW-NB15-v2 and NF-CSE-CIC-IDS2018-v2. These are both updated versions of existing NIDS datasets that have been standardised into a NetFlow format [28] by Sarhan *et al.* [29]. Further details on each dataset are as follows:

- NF-UNSW-NB15-v2
NetFlow formatted version of UNSW-NB15 [30] with 43 standardised features. Out of the 2,390,275 flows, 2,295,222 (96.02%) samples are benign flows and the remaining 95,053 (3.96%) samples are attack flows. 9 attack types are distributed across the 3.98% of flows representing attacks.
- NF-CSE-CIC-IDS2018-v2
Adapted from the CSE-CIC-IDS2018 [31], this dataset contains 18,893,708 flows distributed between 16,635,567 (88.05%) benign samples and 2,258,141 (11.95%) attack samples. Within the 11.95% of attack samples are 6 different attack methods.

Non-contamination experiments omit all non-benign samples during training, whereas 4% of non-benign samples are included for both datasets in contamination experiments. This is due to NF-UNSW-NB15-v2 having a natural attack contamination of approximately 4%. Therefore, to ensure experimental

equality, NF-CSE-CIC-IDS2018-v2 was matched in contamination.

5.2. NF-UNSW-NB15-v2 Results

Table 1 presents results of the experiments on NF-UNSW-NB15-v2 without dataset contamination in terms of Accuracy (Acc), Macro F1-Score (Macro F1) and Detection Rate (DR). The results clearly display the benefit of using Anomal-E embeddings across each performance metric and for each anomaly detection algorithm. In particular, the Macro F1-scores seen in Figure 5 clearly display the significant improvement of using Anomal-E embeddings over raw features, across all anomaly detection methods. For example, when using raw embeddings, a score of only 0.7134 is achieved in the best case. This strongly establishes the benefit of using Anomal-E for network anomaly detection.

Table 1: NF-UNSW-NB15-v2 Results (0% Contamination)

	Raw Features			Embeddings		
	Acc	Macro F1	DR	Acc	Macro F1	DR
PCA	94.45%	70.99%	56.87%	97.64%	83.59%	64.20%
IF	89.64%	66.37%	81.17%	97.91%	85.62%	68.76%
CBLOF	94.12%	68.48%	49.37%	97.70%	84.17%	65.97%
HBOS	94.47%	71.34%	58.24%	98.18%	88.45%	80.36%

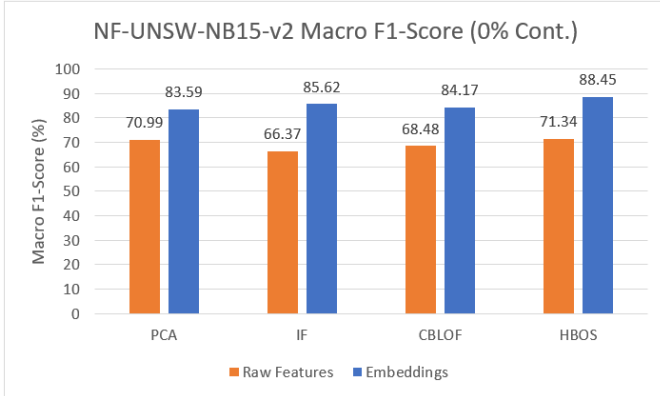


Figure 5: NF-UNSW-NB15-v2 Macro F1-Score (0% Contamination) Comparison

Results for NF-UNSW-NB15-v2 with dataset contamination are presented in Table 2, with Macro F1-Scores visualised in Figure 6. A similar trend can be seen to those presented in the non-contamination version of experiments. The use of raw features causes Macro F1-Scores and detection rates to be significantly lower than scores seen through the use of Anomal-E embeddings. Again, embeddings achieve consistently higher results against all metrics across all detection algorithms. It can also be seen that for raw features, the average Macro F1-Score across the used anomaly detection algorithms is lower than the equivalent experimental results using no contamination. In contrast, the use of Anomal-E embeddings achieves consistently high results for all algorithms, and even improves on embeddings results seen in non-contamination experiments. Again,

this demonstrates the power and benefit of Anomal-E and the leveraging of graph structure in anomaly detection compared to using only raw features.

Table 2: NF-UNSW-NB15-v2 Results (4% Contamination)

	Raw Features			Embeddings		
	Acc	Macro F1	DR	Acc	Macro F1	DR
PCA	91.11%	65.64%	63.01%	98.63%	92.18%	97.86%
IF	91.46%	67.03%	67.60%	98.66%	92.35%	98.77%
CBLOF	95.28%	71.73%	50.42%	98.57%	91.70%	95.72%
HBOS	91.59%	66.90%	65.67%	98.62%	91.89%	94.92%

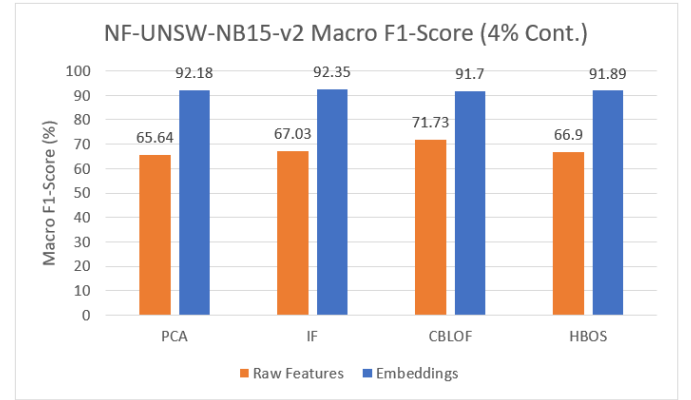


Figure 6: NF-UNSW-NB15-v2 Macro F1 (4% Contamination) Comparison

5.3. NF-CSE-CIC-IDS2018-v2 Results

Similarly to the NF-UNSW-NB15-v2 results, Table 3 displays results for anomaly detection on NF-CSE-CIC-IDS2018-v2 without dataset contamination. In all anomaly detection algorithms, Anomal-E embeddings outperform raw features for accuracy and Macro F1-Score as seen in Figure 7. The overall level and consistency in improvements when using Anomal-E embeddings over raw features clearly demonstrates the benefit of Anomal-E's ability to leverage graph structure for network anomaly detection with no contamination. High detection rates and accuracy in conjunction with Anomal-E's self-supervised training methodology also display the potential this approach has in detecting network anomalies in a range of dynamic environments.

Table 3: NF-CSE-CIC-IDS2018-v2 Results (0% Contamination)

	Raw Features			Embeddings		
	Acc	Macro F1	DR	Acc	Macro F1	DR
PCA	88.30%	76.84%	75.13%	97.82%	94.43%	82.67%
IF	92.06%	81.77%	70.82%	98.18%	95.39%	85.38%
CBLOF	94.42%	87.41%	82.78%	97.83%	94.44%	82.67%
HBOS	94.01%	86.28%	79.28%	97.72%	94.51%	88.55%

For results gathered using NF-CSE-CIC-IDS2018-v2 with dataset contamination, shown in Table 4, we observe that again,

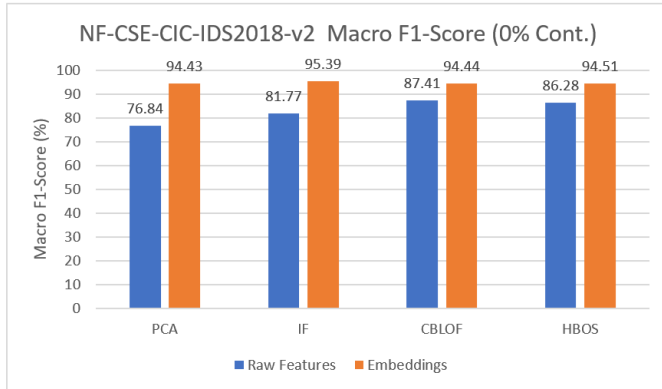


Figure 7: NF-CSE-CIC-IDS2018-v2 Macro F1 (0% Contamination) Comparison

Anomal-E embeddings outperform raw features and clearly display significant increases for all algorithms when contaminating the NF-CSE-CIC-IDS2018-v2 dataset. In a similar fashion to observations made from contaminated experiments on NF-UNSW-NB15-v2, the average scores across performance metrics and detection algorithms are worse for raw features compared to their non-contaminated counterpart. We also observe that not only do Anomal-E embeddings outperform raw features in contaminated experiments, but they also outperform results from non-contaminated Anomal-E embeddings. On average, significant improvements are seen across all 3 performance metrics. Again, this is emphasising the strong potential Anomal-E has for detecting network anomalies in an unsupervised and graph-based learning environment.

Table 4: NF-CSE-CIC-IDS2018-v2 Results (4% Contamination)

	Raw Features			Embeddings		
	Acc	Macro F1	DR	Acc	Macro F1	DR
PCA	85.91%	73.76%	74.71%	97.11%	92.57%	79.16%
IF	86.1%	74.09%	75.39%	89.79%	81.11%	91.84%
CBLOF	94.61%	86.18%	69.16%	97.80%	94.38%	82.67%
HBOS	88.81%	78.82%	84.22%	96.86%	91.89%	77.79%

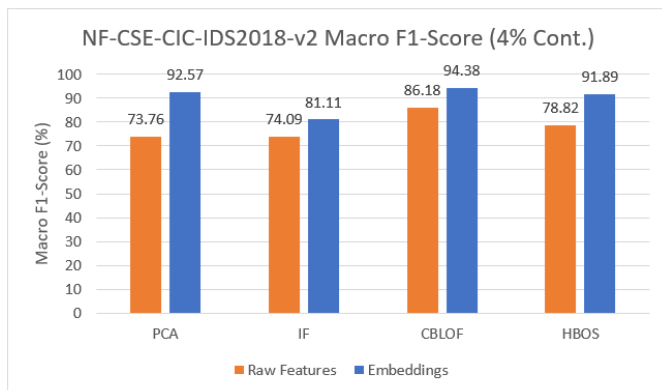


Figure 8: NF-CSE-CIC-IDS2018-v2 Macro F1 (4% Contamination) Comparison

6. Conclusion

To summarise, we present Anomal-E, a self-supervised GNN that incorporates and leverages edge features for network intrusion and anomaly detection. Because of this, Anomal-E has the ability to generalise and adapt to new, sophisticated attack in both artificial and natural network environments. To the best of our knowledge, this is the first approach to network intrusion detection utilising these factors for learning and evaluation. Through our experimental analysis and evaluation of the model, we clearly establish the benefit of using Anomal-E embeddings in attack identification and further solidify this by comparing the improvement to raw feature in 2 benchmark NIDS datasets. This also further demonstrates the capabilities and potential of self-supervised GNNs for NIDSs. Moving forward, we plan to evaluate Anomal-E using real network traffic to gather informative insights into model performance outside of synthetic datasets. We also plan on investigating the effects of temporal-based training to further the exploration into Anomal-E’s performance outside synthetic network conditions.

References

- [1] Z. Wu, S. Pan, F. Chen, G. Long, C. Zhang, S. Y. Philip, A comprehensive survey on graph neural networks, *IEEE transactions on neural networks and learning systems* 32 (1) (2020) 4–24.
- [2] W. L. Hamilton, R. Ying, J. Leskovec, Inductive representation learning on large graphs, in: *Proceedings of the 31st International Conference on Neural Information Processing Systems*, 2017, pp. 1025–1035.
- [3] A. Grover, J. Leskovec, node2vec: Scalable feature learning for networks, in: *Proceedings of the 22nd ACM SIGKDD international conference on Knowledge discovery and data mining*, 2016, pp. 855–864.
- [4] W. W. Lo, S. Layeghy, M. Sarhan, M. Gallagher, M. Portmann, E-graphsage: A graph neural network based intrusion detection system for iot, in: *NOMS 2022-2022 IEEE/IFIP Network Operations and Management Symposium*, 2022, pp. 1–9. doi:10.1109/NOMS54207.2022.9789878.
- [5] P. Veličković, W. Fedus, W. L. Hamilton, P. Liò, Y. Bengio, R. D. Hjelm, Deep Graph Infomax, in: *International Conference on Learning Representations*, 2019. URL <https://openreview.net/forum?id=rklz9iAcKQ>
- [6] F. T. Liu, K. M. Ting, Z.-H. Zhou, Isolation forest, in: *2008 eighth IEEE international conference on data mining*, IEEE, 2008, pp. 413–422.
- [7] M.-L. Shyu, S.-C. Chen, K. Sarinapakorn, L. Chang, A novel anomaly detection scheme based on principal component classifier, Tech. rep., Miami Univ Coral Gables FI Dept of Electrical and Computer Engineering (2003).
- [8] Z. He, X. Xu, S. Deng, Discovering cluster-based local outliers, *Pattern recognition letters* 24 (9-10) (2003) 1641–1650.
- [9] M. Goldstein, A. Dengel, Histogram-based outlier score (hbos): A fast unsupervised anomaly detection algorithm, *KI-2012: poster and demo track* 9.
- [10] P. Casas, J. Mazel, P. Owezarski, Unsupervised network intrusion detection systems: Detecting the unknown without knowledge, *Computer Communications* 35 (7) (2012) 772–783.
- [11] I. Syarif, A. Prugel-Bennett, G. Wills, Unsupervised clustering approach for network anomaly detection, in: *International conference on networked digital technologies*, Springer, 2012, pp. 135–145.
- [12] L. Leichtnam, E. Totel, N. Prigent, L. Mé, Sec2graph: Network attack detection based on novelty detection on graph structured data, in: *International Conference on Detection of Intrusions and Malware, and Vulnerability Assessment*, Springer, 2020, pp. 238–258.
- [13] M. H. Bhuyan, D. Bhattacharyya, J. K. Kalita, An effective unsupervised network anomaly detection method, in: *Proceedings of the international conference on advances in computing, communications and informatics*, 2012, pp. 533–539.

- [14] S. Layeghy, M. Portmann, On generalisability of machine learning-based network intrusion detection systems (2022). doi:10.48550/ARXIV.2205.04112.
URL <https://arxiv.org/abs/2205.04112>
- [15] M. Lopez-Martin, B. Carro, J. I. Arribas, A. Sanchez-Esguevillas, Network intrusion detection with a novel hierarchy of distances between embeddings of hash ip addresses, *Knowledge-Based Systems* 219 (2021) 106887.
- [16] Q. Xiao, J. Liu, Q. Wang, Z. Jiang, X. Wang, Y. Yao, Towards Network Anomaly Detection Using Graph Embedding, in: V. V. Krzhizhanovskaya, G. Závodszy, M. H. Lees, J. J. Dongarra, P. M. A. Sloot, S. Brissos, J. Teixeira (Eds.), *Computational Science – ICCS 2020*, Springer International Publishing, Cham, 2020, pp. 156–169.
- [17] W. L. Hamilton, R. Ying, J. Leskovec, Inductive representation learning on large graphs, in: *Advances in Neural Information Processing Systems*, 2017. arXiv:1706.02216.
- [18] J. Zhou, Z. Xu, A. M. Rush, M. Yu, Automating botnet detection with graph neural networks, arXiv preprint arXiv:2003.06344.
- [19] S. Nagaraja, P. Mittal, C.-Y. Hong, M. Caesar, N. Borisov, Botgrep: Finding p2p bots with structured graph analysis, in: *19th USENIX Security Symposium (USENIX Security 10)*, USENIX Association, Washington, DC, 2010.
URL <https://www.usenix.org/conference/usenixsecurity10/botgrep-finding-p2p-bots-structured-graph-analysis>
- [20] L. Chang, P. Branco, Graph-based solutions with residuals for intrusion detection: the modified e-graphsage and e-resgat algorithms, arXiv preprint arXiv:2111.13597.
- [21] J. Zhou, G. Cui, S. Hu, Z. Zhang, C. Yang, Z. Liu, L. Wang, C. Li, M. Sun, Graph neural networks: A review of methods and applications, *AI Open* 1 (2020) 57–81.
- [22] K. Xu, W. Hu, J. Leskovec, S. Jegelka, How powerful are graph neural networks?, arXiv preprint arXiv:1810.00826.
- [23] H. Cai, V. W. Zheng, K. C.-C. Chang, A comprehensive survey of graph embedding: Problems, techniques, and applications, *IEEE Transactions on Knowledge and Data Engineering* 30 (9) (2018) 1616–1637.
- [24] J. Zhou, G. Cui, S. Hu, Z. Zhang, C. Yang, Z. Liu, L. Wang, C. Li, M. Sun, Graph neural networks: A review of methods and applications, *AI Open* 1 (2020) 57–81. doi:<https://doi.org/10.1016/j.aiopen.2021.01.001>.
URL <https://www.sciencedirect.com/science/article/pii/S2666651021000012>
- [25] W. W. Lo, S. Layeghy, M. Portmann, Inspection-I: Practical gnn-based money laundering detection system for bitcoin, arXiv preprint arXiv:2203.10465.
- [26] P. Veličković, W. Fedus, W. L. Hamilton, P. Liò, Y. Bengio, R. D. Hjelm, Deep graph infomax, *International Conference on Learning Representations (ICLR)*.
- [27] A. Singla, E. Bertino, D. Verma, Preparing network intrusion detection deep learning models with minimal data using adversarial domain adaptation, in: *Proceedings of the 15th ACM Asia Conference on Computer and Communications Security*, 2020, pp. 127–140.
- [28] B. Claise, Cisco Systems NetFlow Services Export Version 9, RFC 3954 (Oct. 2004). doi:10.17487/RFC3954.
URL <https://rfc-editor.org/rfc/rfc3954.txt>
- [29] M. Sarhan, S. Layeghy, M. Portmann, Towards a standard feature set for network intrusion detection system datasets, *Mobile Networks and Applications* 27 (1) (2022) 357–370.
- [30] N. Moustafa, J. Slay, Unsw-nb15: a comprehensive data set for network intrusion detection systems (unsw-nb15 network data set), in: *2015 Military Communications and Information Systems Conference (MilCIS)*, 2015, pp. 1–6. doi:10.1109/MilCIS.2015.7348942.
- [31] I. Sharafaldin., A. Habibi Lashkari., A. A. Ghorbani., Toward generating a new intrusion detection dataset and intrusion traffic characterization, in: *Proceedings of the 4th International Conference on Information Systems Security and Privacy - ICISPP, INSTICC, SciTePress*, 2018, pp. 108–116. doi:10.5220/0006639801080116.